Minimum-Time Optimal Control of Many Robots that Move in the Same Direction at Different Speeds

Timothy Bretl, *Member, IEEE*

***Abstract*—In this paper, we solve the minimum-time optimal control problem for a group of robots that can move at different speeds but that must all move in the same direction. We are motivated to solve this problem because constraints of this sort are common in micro-scale and nano-scale robotic systems. By application of the minimum principle, we obtain necessary conditions for optimality and use them to guess a candidate control policy. By showing that the corresponding value function is a viscosity solution to the Hamilton–Jacobi–Bellman equation, we verify that our guess is optimal. The complexity of finding this policy for arbitrary initial conditions is only quasilinear in the number of robots, and in fact is dominated by the computation of a planar convex hull. We extend this result to consider obstacle avoidance by explicit parameterization of all possible optimal control policies, and show examples in simulation.**

***Index Terms*—Motion planning, multi-robot systems, optimal control.**

I. Introduction

In this paper, we will solve the minimum-time optimal control problem for a group of n robots that can move in a planar workspace at different (although bounded) speeds, but that must all move in the same direction. Fig. 1 shows an example result for $n = 3$ robots that already hints at the beautiful geometric nature of the solution to this problem. We will show that the trajectory in this example is optimal, and that the algorithm applied to generate it (see Fig. 2) is correct.

We are motivated to solve this problem because the operating constraint is exactly the one exhibited by a particular microrobotic system, the "MagMite," that was developed recently by researchers at ETH-Zurich [1]–[6]. This system is controlled by an external magnetic field. Rotating the field rotates the robot, while oscillating the field drives the robot to resonance and propels it forward. Many robots can be driven at the same time at different speeds, as long as each one has a different resonant frequency. However, all robots must move in the same direction.

Similar constraints, requiring that some control inputs be the same for all robots, arise in many other micro/nano-scale systems [7]. Specific examples include the untethered scratch-drive actuator [8] and the "Mag-μBot" [9], [10], where the common challenge is to somehow differentiate each robot's response. The standard way to deal with this challenge has been to decouple robots through hardware modification. For example, the work of [11], [12] uses electromechanical hysteresis to make particular scratch-drive actuators respond to some control inputs but not to others. A similar approach is taken by [13], which uses a structured electrostatic substrate to selectively immobilize Mag-μBots. Our approach here is quite different, where we ask what can be done with the appropriate choice of control algorithm. It extends a line of thinking that began in our own earlier work [14]–[16], and is most closely related to the notion of "broadcast feedback" and stochastic recruitment control in robotics [17], [18] and to ensemble control theory in applied mathematics [19], [20].

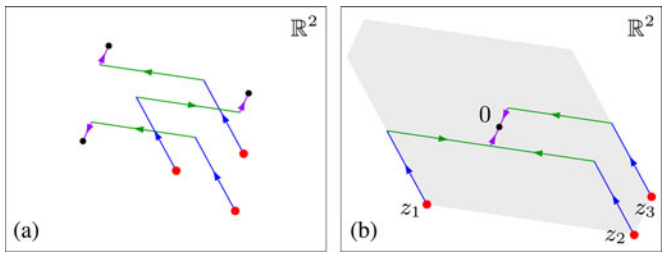

Fig. 1. (a) Minimum-time optimal trajectory for three robots with bounded speed in a planar workspace, under the constraint that all robots move in the same direction. (b) The same trajectory translated so each goal is at the origin, showing its relationship to the convex hull of $\{z_1, z_2, z_3, -z_1, -z_2, -z_3\}$.

The minimum-time optimal control problem that we will solve is stated formally as follows:

$$\begin{aligned} &\text{minimize} && \int_0^{t_f} dt \\ &\text{subject to} && \left.\begin{aligned} \dot{x}_i &= v_i \begin{bmatrix} \cos u \\ \sin u \end{bmatrix} \\ |v_i| &\leq 1 \end{aligned}\right\} \text{ for } i \in \{1, \ldots, n\} \end{aligned} \tag{1}$$

with boundary conditions

$$\left.\begin{aligned} x_i(0) &= z_i \\ x_i(t_f) &= 0 \end{aligned}\right\} \text{ for } i \in \{1, \ldots, n\} \tag{2}$$

and free final time t_f, where the state is

$$x = (x_1, \ldots, x_n) \in \mathbb{R}^2 \times \cdots \times \mathbb{R}^2$$

and the inputs are $u \in [-\pi, \pi)$ and

$$v = (v_1, \ldots, v_n) \in \mathbb{R} \times \cdots \times \mathbb{R}.$$

Manuscript received February 7, 2011; revised August 9, 2011; accepted October 13, 2011. Date of publication November 24, 2011; date of current version April 9, 2012. This paper was recommended for publication by Associate Editor D. Hsu and Editor G. Oriolo upon evaluation of the reviewers' comments. This work was supported by the National Science Foundation under CPS-0931871 and Grant CMMI-0956362.

T. Bretl is with the Department of Aerospace Engineering, University of Illinois at Urbana-Champaign, Urbana, IL, 61801, USA (e-mail: tbretl@illinois.edu).

Color versions of one or more of the figures in this paper are available online at http://ieeexplore.ieee.org.

Digital Object Identifier 10.1109/TRO.2011.2173235

Our assumption that $x_i(t_f) = 0$ is for convenience. Trajectories of (1) are invariant under translation, so arbitrary boundary conditions $x_i(0) = a_i$ and $x_i(t_f) = b_i$ are achieved by taking $z_i = a_i - b_i$. This model captures the key constraint on the "MagMite" in [1]–[6] that makes control of this microrobotic system hard, at least from an algorithmic point of view.

We will begin in the classical way by applying the minimum principle of Pontryagin [21] to obtain necessary conditions for optimality, and using these conditions to guess a candidate control policy (see Section II). To verify that our guess is optimal, the usual next step would be establishing a regular synthesis [22] or appealing to geometric arguments—for example, see the seminal work to derive Dubins [23], Reeds-Shepp [24], or Balkcom-Mason [25] curves for car-like vehicles. We will be required instead to provide sufficient conditions by showing that the value function corresponding to our candidate control policy is a viscosity solution to the Hamilton-Jacobi-Bellman equation (see Section III). In doing so, we follow an approach that has so far been taken more often in control theory and applied mathematics [26], [27] than in robotics. We will apply the resulting optimal control algorithm (see Fig. 2) to several examples in simulation (see Section IV).

Beyond the intended application to a particular microrobotic system, three aspects of our solution to the optimal control problem (1)–(2) merit particular interest:

1) We will show that the time required to compute a solution to (1)–(2) is only $O(n \log n)$, and in particular is dominated by the computation of a planar convex hull. This result is surprising, and suggests the existence of hidden structure in planning and control problems for large groups of micro/nano-scale robots (as well as for related systems like the one considered in [16]) that may vastly simplify these problems.
2) We will show that, in worst case, the solution to (1)–(2) has cost

$$t_f = \frac{\pi}{2} \left(\max_{i \in \{1,\ldots,n\}} \|z_i\| \right),$$

where $\|\cdot\|$ is the standard Euclidean distance metric. If each robot was free to move in any direction, this cost would instead be

$$t_f = \max_{i \in \{1,\ldots,n\}} \|z_i\|.$$

As a consequence, with respect to our model, the design compromise that couples the movement direction of the microrobots in [1]–[6] only makes these robots $\pi/2$ times slower in worst case. This result is useful when deciding if it is worth the effort to eliminate coupling through further hardware modification.
3) We will show that the solution to (1)-(2) is not unique, and in particular we will show how to explicitly construct the space of all possible optimal trajectories. This space is reminiscent of the "task-completion diagram" or "coordination space" that has been used in multi-robot motion planning [28]–[30]. It will allow us to consider obstacle avoidance (including collisions between robots) while retaining a guarantee of optimality.

We will discuss the extent to which these results generalize, and in particular the extent to which they can be applied to real robots, in our concluding remarks (see Section V).

Finally, note that we studied a similar model of the same robotic system [1]–[6] in our own previous work, presented at a conference [31]. However, in that work, we considered a different cost function and took a heuristic solution approach.

II. Necessary Conditions

A. The Form of the Hamiltonian

Consider the minimum-time optimal control problem (1)–(2) that was posed in Section I. We will abbreviate

$$\widehat{u} = \begin{bmatrix} \cos u \\ \sin u \end{bmatrix}$$

for any $u \in [-\pi, \pi)$, so the dynamic model will be expressed as

$$\dot{x}_i = v_i \widehat{u}, \qquad \text{for } i \in \{1, \ldots, n\}.$$

Since $\widehat{u} = -\widehat{u + \pi}$, we can restrict $u \in [0, \pi)$ without loss of generality. The Hamiltonian associated with (1) is

$$H(x, p, u, v) = 1 + \sum_{i=1}^{n} p_i^T \left(v_i \widehat{u} \right), \tag{3}$$

where

$$p = (p_1, \ldots, p_n) \in \mathbb{R}^2 \times \cdots \times \mathbb{R}^2$$

is the costate. The minimum principle [21], [32] tells us that along any optimal trajectory (x^*, p^*, u^*, v^*), we must have

$$-\dot{p}^* = \nabla_x H(x^*, p^*, u^*, v^*) \tag{4}$$

and

$$0 = H(p^*, x^*, u^*, v^*) \tag{5a}$$

$$\leq \min_{u,v} H(p^*, x^*, u, v). \tag{5b}$$

Since the Hamiltonian (3) has no dependence on the state, the condition (4) implies that the costate is constant in time:

$$p_i(t) = p_i(0) \equiv p_i, \qquad \text{for } i \in \{1, \ldots, n\}.$$

Similarly, the condition (5) leads to the following result:

Lemma 1: The Hamiltonian (3) has the form

$$H(x, p, u, v) = 1 - \sum_{i=1}^{n} \left| p_i^T \widehat{u} \right|$$

along any optimal trajectory.

Proof: If $p_i^T \widehat{u} = 0$, then $v_i \left(p_i^T \widehat{u} \right) = 0$. If $p_i^T \widehat{u} \neq 0$, then the condition (5b) requires that

$$v_i = -\text{sign} \left(p_i^T \widehat{u} \right).$$

Together, these two facts imply that

$$v_i \left(p_i^T \widehat{u} \right) = - \left| p_i^T \widehat{u} \right|$$

for $i \in \{1, \ldots, n\}$ and $u \in [0, \pi)$. Our result follows. ∎

B. Minimizing the Hamiltonian

In the previous section, we showed that the Hamiltonian is a function only of the heading angle u. In this section, we will show that at least one and at most n values of u minimize the Hamiltonian. We will immediately be able to conclude that $u(t)$ is piecewise-constant and takes on at most n values along any optimal trajectory. Before proving our main result (see Lemma 3), we will require a key fact about the geometrical relationship between p_i and $\widehat{u}$ at any minimizing angle u (see Lemma 2), which itself is based on some results from real analysis that are collected in the Appendix (see Lemmas 11-13).

Lemma 2: The Hamiltonian

$$H(u) = 1 - \sum_{i=1}^{n} \left| p_i^T \widehat{u} \right| \tag{6}$$

has no minimum at any $u_0 \in [0, \pi)$ satisfying both $p_i \neq 0$ and $p_i^T \widehat{u_0} = 0$ for some $i \in \{1, \ldots, n\}$.

Proof: Assume to the contrary that such a u_0 exists. Define the index set

$$\mathcal{I} = \left\{ i \in \{1, \ldots, n\} : p_i^T \widehat{u_0} = 0 \right\}$$

and let $\mathcal{J} = \{1, \ldots, n\} \setminus \mathcal{I}$.

First, we will show that $\mathcal{J}$ is non-empty. If we assume the contrary, then $H(u_0) = 1$. The minimum principle requires that the costate never vanish, i.e., that $p_k \neq 0$ for some $k \in \{1, \ldots, n\}$. It is always possible to choose $u \in [0, \pi)$ such that $\widehat{u} = p_k / \|p_k\|$, hence that

$$1 - \sum_{i=1}^{n} \left| p_i^T \widehat{u} \right| = 1 - \|p_k\| - \sum_{\substack{i=1 \\ i \neq k}}^{n} \left| p_i^T \widehat{u} \right| < 1.$$

As a consequence, it must be the case that

$$\min_{u \in [-\pi, \pi)} 1 - \sum_{i=1}^{n} \left| p_i^T \widehat{u} \right| < 1 = H(u_0),$$

contradicting the assumption that u_0 minimizes (6). So, we conclude that $\mathcal{J}$ is non-empty, as desired.

Next, we note that

$$\sum_{i \in \mathcal{I}} \left| p_i^T \widehat{u} \right| = \left| \sum_{i \in \mathcal{I}} p_i^T \widehat{u} \right|.$$

This result follows immediately from the fact that for all $i, j \in \mathcal{I}$ there exists some $c \in \mathbb{R}$ such that $p_i = c p_j$.

Finally, we define two functions

$$g(u) = \sum_{i \in \mathcal{I}} p_i^T \widehat{u} \qquad \text{and} \qquad h(u) = \sum_{i \in \mathcal{J}} \left| p_i^T \widehat{u} \right|,$$

noting that both g and h are differentiable at u_0 and that

$$g(u_0) = 0, \qquad \frac{dg}{du}(u_0) \neq 0.$$

We can show (see the Appendix, Lemma 13) that $f(u) = |g(u)| + h(u)$ has no maximum at u_0, hence that $H(u) = 1 - f(u)$ has no minimum at u_0, and so we have our result. ■

Lemma 3: There are at least one and at most n points in $[0, \pi)$ at which the Hamiltonian

$$H(u) = 1 - \sum_{i=1}^{n} \left| p_i^T \widehat{u} \right|$$

is minimized.

Proof: First, since the function H is continuous and real-valued, then it must have a minimum on the interval $[0, \pi]$. Since H is periodic in π, then it must have the same minimum on $[0, \pi)$, completing the first part of our proof.

Next, we define the index set

$$\mathcal{I} = \{ i \in \{1, \ldots, n\} : p_i = 0 \}$$

and let $\mathcal{J} = \{1, \ldots, n\} \setminus \mathcal{I}$. We know from Lemma 2 that $p_i^T \widehat{u} \neq 0$ for all $i \in \mathcal{J}$ at any point u that minimizes H, and that $\mathcal{J}$ is non-empty. As a consequence, we may write

$$H(u) = 1 - \sum_{i \in \mathcal{J}} \left| p_i^T \widehat{u} \right|$$

and note that H is differentiable at any such point, giving us the following necessary condition:

$$\begin{aligned} 0 = \frac{dH}{du} &= \sum_{i \in \mathcal{J}} \left(p_i^T R \widehat{u} \right) \operatorname{sign} \left(p_i^T \widehat{u} \right) \\ &= \left(\sum_{i \in \mathcal{J}} \operatorname{sign} \left(p_i^T \widehat{u} \right) p_i^T R \right) \widehat{u} \\ &= q(u)^T \widehat{u}, \end{aligned}$$

where we have defined the rotation matrix

$$R = \begin{bmatrix} 0 & 1 \\ -1 & 0 \end{bmatrix}$$

and the parameter vector

$$q(u) = \left(\sum_{i \in \mathcal{J}} \operatorname{sign} \left(p_i^T \widehat{u} \right) p_i^T R \right)^T.$$

Denote the number of elements in $\mathcal{J}$ by m. Each term $p_i^T \widehat{u}$ has exactly one zero crossing in $[0, \pi)$ and both H and dH/du are periodic in π, so q takes on at most m values in $[0, \pi)$. At a particular value of q, dH/du is a sinusoid with at most one zero crossing in $[0, \pi)$. Hence, dH/du has at most m zero crossings in $[0, \pi)$, and so H has at most m minima, where we note that $m \leq n$, as desired.

We may confirm that these are minima (rather than maxima) by noting that

$$\frac{d^2 H}{du^2} = \sum_{i \in \mathcal{J}} \left| p_i^T \widehat{u} \right| > 0$$

on intervals of constant q. ■

C. Structure of an Optimal Trajectory

In the previous section, we showed that the heading angle u takes on at most n distinct values along any optimal trajectory. In this section, we will show that each value of u

need be applied exactly once, i.e., that no "chattering" need occur. In doing so, we will have transformed (1)-(2) from an infinite-dimensional problem, in which we are required to specify functions $u(t) : [0, t_f] \to [0, \pi)$ and $v_i : [0, t_f] \to [-1, 1]$ for $i \in \{1, \ldots, n\}$, into a finite-dimensional problem, in which we are required only to specify a sequence of n values of u.

Lemma 4: Given any solution to (1)-(2), we may construct another solution of the form

$$\left.\begin{array}{l} u(t) = U_j \\ v_i(t) = V_{ij} \end{array}\right\} \quad \text{for} \quad \sum_{k=1}^{j-1} T_k \leq t < \sum_{k=1}^{j} T_k.$$

for $i \in \{1, \ldots, n\}$, where $T \in \mathbb{R}^m$, $U \in [0, \pi)^m$, and $V \in [-1, 1]^{n \times m}$, and where $1 \leq m \leq n$. We denote this solution by the tuple (T, U, V) and say that it has m steps.

Proof: First, we note that $u(t)$ is piecewise-constant, as an immediate consequence of Lemma 3. In particular, we know that $u(t)$ takes on m values in $[0, \pi)$, where $1 \leq m \leq n$. Denote these values by $U_1, \ldots, U_m$.

Next, given any solution to (1)-(2), we will show how to construct another solution in which each input U_j is applied exactly once, for a time interval of some length T_j. Consider an arbitrary time interval $[t_0, t_1] \subset [0, t_f]$. Define new inputs $u'(t) = u(r(t))$ and $v_i'(t) = v_i(r(t))$, where the function

$$r(t) = \begin{cases} t_0 + t_1 - t, & \text{if } t \in [t_0, t_1] \\ t, & \text{otherwise} \end{cases}$$

simply reverses the flow of time on this interval. Then

$$\begin{aligned} x_i'(t_1) - x_i'(t_0) &= \int_{t_0}^{t_1} v_i'(t)\widehat{u'(t)}dt \\ &= \int_{t_0}^{t_1} v_i(r(t))\widehat{u(r(t))}dt \\ &= \int_{t_0}^{t_1} v_i(s)\widehat{u(s)}ds \\ &= x_i(t_1) - x_i(t_0). \end{aligned}$$

Changing the order in which intervals of constant $u(t)$ are applied evidently leaves both t_f and $x_i(t_f)$ invariant, so our result follows.

Finally, we note that $v_i(t)$ for each $i \in \{1, \ldots, n\}$ can be expressed in the required form, simply by replacing it with its average value over intervals of constant $u(t)$. In particular, for each $j \in \{1, \ldots, m\}$, we define

$$V_{ij} = \frac{1}{t_1 - t_0} \int_{t_0}^{t_1} v_i(t)dt$$

where

$$t_0 = \sum_{k=1}^{j-1} T_k, \qquad t_1 = \sum_{k=1}^{j} T_k.$$

Then, the input

$$v_i'(t) = V_{ij}, \quad \text{for} \quad \sum_{k=1}^{j-1} T_k \leq t < \sum_{k=1}^{j} T_k$$

produces exactly the same result as $v_i(t)$. ∎

Note that the time cost of an m-step trajectory (T, U, V) is simply $T_1 + \cdots + T_m$. Note also that if $p_i \neq 0$, then we have

$$V_{ij} = -\text{sign}\left(p_i^T \widehat{U_j}\right).$$

If instead $p_i = 0$, then the optimal choice of V_{ij} is still unclear. The next section will shed light on this question.

D. Invariance of the Optimal Trajectory

In the previous section, we showed that any optimal trajectory is equivalent to one in which $u(t)$ is piecewise-constant and takes a sequence of m distinct values $U_1, \ldots, U_m \in [0, \pi)$, where $1 \leq m \leq n$. In this section we will suggest how to choose these m values. We proceed by noting that this choice evidently depends only on a subset of robots, in particular on each robot i with which we must associate a non-zero costate $p_i \neq 0$. We will characterize this subset, showing that $p_i \neq 0$ only if the initial position z_i is a vertex of the convex hull

$$\text{conv}\left(\{z_1, \ldots, z_n, -z_1, \ldots, -z_n\}\right)$$

which you will recall from the example of Fig. 1. This result is a consequence of Lemma 5, which will show that robots can be added without changing the optimal trajectory as long as they begin inside this convex hull. Our proof will be constructive, and in fact will give an explicit formula for an optimal choice of V_{ij}, clearing up a question raised above. As a corollary, Lemma 5 leaves us with a good guess at the optimal choice of $U_1, \ldots, U_m$—namely, oriented along edges of the hull. We will see in the following section that this guess is correct.

Lemma 5: Assume that (T, U, V) is an m-step solution to the optimal control problem (1)–(2) for n robots satisfying $x_i(0) = z_i$ for all $i \in \{1, \ldots, n\}$. Let

$$z_{n+1} = \sum_{i=1}^{n} (a_i - b_i) z_i$$

for any $a_1, \ldots, a_n \geq 0$ and $b_1, \ldots, b_n \geq 0$ satisfying

$$1 = \sum_{i=1}^{n} (a_i + b_i).$$

Then (T, U, V') is an m-step solution to (1)–(2) with exactly the same cost for $n + 1$ robots, where $x_{n+1}(0) = z_{n+1}$ and

$$V_{ij}' = \begin{cases} V_{ij}, & i \in \{1, \ldots, n\} \\ \sum_{k=1}^{n} (a_k - b_k) V_{kj}, & i = n + 1. \end{cases}$$

Also, if p and (T, U, V) satisfy the necessary conditions (4)-(5), then so do p' and (T, U, V'), where

$$p_i' = \begin{cases} p_i, & i \in \{1, \ldots, n\} \\ 0, & i = n + 1. \end{cases}$$

Proof: It is clear that (T, U, V') steers the original n robots to the origin with no increase in cost, and that the presence of robot $n + 1$ cannot possibly decrease this cost. This trajectory also steers robot $n + 1$ to the origin:

$$x_{n+1}\left(\sum_{j=1}^{m} T_j\right) = z_{n+1} + \sum_{j=1}^{m} T_j V_{n+1,j}' \widehat{U_j}$$

$$
\begin{aligned}
&= z_{n+1} + \sum_{j=1}^{m} T_j \sum_{i=1}^{n} (a_i - b_i)\, V_{ij} \widehat{U_j} \\
&= z_{n+1} + \sum_{i=1}^{n} (a_i - b_i) \sum_{j=1}^{m} T_j V_{ij} \widehat{U_j} \\
&= z_{n+1} - \sum_{i=1}^{n} (a_i - b_i)\, z_i \\
&= 0.
\end{aligned}
$$

Since each $V'_{n+1,j}$ is a convex combination of $V_{1j}, \ldots, V_{nj}$ and since $|V_{ij}| \leq 1$ for all $i \in \{1, \ldots, n\}$ and $j \in \{1, \ldots, m\}$ by assumption, then we must also have $\left|V'_{n+1,j}\right| \leq 1$ for all $j \in \{1, \ldots, m\}$. So, (T, U, V') is a solution to (1)–(2).

Finally, if we choose $p'_{n+1} = 0$, then we leave the Hamiltonian unchanged, so Lemma 1 implies that (4)–(5) are satisfied by p' and (T, U, V') just as they were by p and (T, U, V). ■

E. Candidate Solution Algorithm

The results of the previous section motivate the candidate solution algorithm OPTIMALCONTROL shown in Fig. 2. This algorithm takes the initial conditions $z_1, \ldots, z_n$ as input, and returns an η-step trajectory (T, U, V), where 2η is equal to the number of vertices in the convex hull

$$\text{conv}\left(\{z_1, \ldots, z_n, -z_1, \ldots, -z_n\}\right).$$

The total cost of this trajectory is simply

$$t_f = \text{perim}\left(\text{conv}\left(\{z_1, \ldots, z_n, -z_1, \ldots, -z_n\}\right)\right)/4.$$

We will show (see Lemma 7) that this trajectory satisfies the minimum principle for the problem (1)-(2). To do so, we will begin with a preliminary result (Lemma 6) that tells us how to construct the required costate p.

Lemma 6: For some $m \leq n$, assume $u_1, \ldots, u_m \in [0, \pi)$ are ordered so that $u_j > u_i$ for all $j > i$. If

$$p_i = \begin{cases} -\left(\widehat{u_m} + \widehat{u_1}\right)/2, & i = 1 \\ \left(\widehat{u_{i-1}} - \widehat{u_i}\right)/2, & i \in \{2, \ldots, m\} \\ 0, & i \in \{m+1, \ldots, n\} \end{cases}$$

then

$$\text{sign}\left(p_i^T \widehat{u_j}\right) = \begin{cases} -1, & i \leq j \\ 1, & i > j \end{cases}$$

and the function

$$H(u) = 1 - \sum_{i=1}^{n} \left|p_i^T \widehat{u}\right|$$

satisfies

$$\{u_1, \ldots, u_m\} = \arg \min_{u \in [0,\pi)} H(u)$$

$$0 = \min_{u \in [0,\pi)} H(u).$$

Proof: First, we show that $H(u_j) = 0$. Notice that

$$1 - \sum_{i=1}^{n} \left|p_i^T \widehat{u}\right| = 1 - \sum_{i=1}^{m} \left|p_i^T \widehat{u}\right|.$$

OPTIMALCONTROL$(z_1, \ldots, z_n)$

Given $z_1, \ldots, z_n \in \mathbb{R}^2$, do the following:

- Find the convex hull
$$\text{conv}\left(\{z_1, \ldots, z_n, -z_1, \ldots, -z_n\}\right)$$
and denote its vertex set by
$$Z = \{\zeta_1, \ldots, \zeta_\eta, -\zeta_1, \ldots, -\zeta_\eta\}.$$
- Find $u_1, \ldots, u_\eta$ satisfying
$$\begin{bmatrix} \cos u_i \\ \sin u_i \end{bmatrix} = \begin{cases} (\zeta_{i+1} - \zeta_i)/\left\|\zeta_{i+1} - \zeta_i\right\| & i < \eta \\ (-\zeta_1 - \zeta_i)/\left\|\zeta_1 + \zeta_i\right\| & i = \eta. \end{cases}$$
Reorder Z so that
$$u_1, \ldots, u_\eta \in [0, \pi)$$
and $u_j > u_i$ for all $j > i$.
- Find $a_{i1}, \ldots, a_{i\eta}, b_{i1}, \ldots, b_{i\eta} \geq 0$ satisfying
$$z_i = \sum_{j=1}^{\eta} (a_{ij} - b_{ij})\, \zeta_j$$
$$1 = \sum_{j=1}^{\eta} (a_{ij} + b_{ij})$$
for all $i \in \{1, \ldots, n\}$.
- Find
$$T_j = \begin{cases} \left\|\zeta_{j+1} - \zeta_j\right\|/2 & j < \eta \\ \left\|\zeta_1 + \zeta_j\right\|/2 & j = \eta \end{cases}$$
$$U_j = u_j$$
$$\Upsilon_{ij} = \begin{cases} 1 & i \leq j \\ -1 & i > j \end{cases}$$
for all $i, j \in \{1, \ldots, \eta\}$ and then find
$$V_{ij} = \sum_{k=1}^{\eta} (a_{ik} - b_{ik})\, \Upsilon_{kj}$$
for all $i \in \{1, \ldots, n\}$ and $j \in \{1, \ldots, \eta\}$.

Return (T, U, V).

Fig. 2. Algorithm that finds a solution to (1)–(2).

For $i = 1$, we compute

$$
\begin{aligned}
\text{sign}\left(p_1^T \widehat{u_j}\right) &= \text{sign}\left(-\left(\frac{\widehat{u_m} + \widehat{u_1}}{2}\right)^T \widehat{u_j}\right) \\
&= -\text{sign}\left(\cos\left(u_m - u_j\right) + \cos\left(u_1 - u_j\right)\right).
\end{aligned}
$$

Since $u_1, \ldots, u_m \in [0, \pi)$, we have

$$\cos\left(u_m - u_j\right) \geq \cos\left(0 - u_j\right) = \cos u_j$$
$$\cos\left(u_1 - u_j\right) > \cos\left(\pi - u_j\right) = -\cos u_j$$

so in fact

$$\cos\left(u_m - u_j\right) + \cos\left(u_1 - u_j\right) > 0.$$

We conclude that sign $\left(p_1^T \widehat{u_j}\right) = -1$. By a similar computation for $i \in \{2, \ldots, m\}$, we find that

$$\text{sign}\left(p_i^T \widehat{u_j}\right) = \begin{cases} -1, & i \leq j \\ 1, & i > j. \end{cases}$$

As a consequence

$$\begin{aligned} H(u_j) &= 1 - \left(-\sum_{i=1}^{j} p_i + \sum_{i=j+1}^{m} p_i \right)^T \widehat{u_j} \\ &= 1 - \widehat{u_j}^T \widehat{u_j} = 0, \end{aligned}$$

as desired.

Next, we show that $H(u_j)$ is a minimum. Following the proof of Lemma 3, we define the rotation matrix

$$R = \begin{bmatrix} 0, & 1 \\ -1, & 0 \end{bmatrix}$$

and compute

$$\begin{aligned} \frac{dH}{du}(u_j) &= \left(-\sum_{i=1}^{j} p_i + \sum_{i=j+1}^{m} p_i \right)^T R\widehat{u_j} \\ &= \widehat{u_j}^T R \widehat{u_j} \\ &= 0 \end{aligned}$$

and

$$\frac{d^2 H}{du^2}(u_j) = \sum_{i=1}^{m} \left| p_i^T \widehat{u_j} \right| > 0,$$

as desired.

Finally, since we have identified m minima and since we know from the proof of Lemma 3 that there are at most m, then no other minima exist, and so we have our result. ∎

Lemma 7: The η-step trajectory (T, U, V) produced by the algorithm OPTIMALCONTROL$(z_1, \ldots, z_n)$ in Fig. 2 satisfies the minimum principle for the problem (1)-(2).

Proof: It suffices to show that (T, U, Υ) satisfies the minimum principle for η robots with initial position $x_i(0) = \zeta_i$ for each $i \in \{1, \ldots, \eta\}$. Our result would then be an immediate consequence of Lemma 5. To do so, we must verify the boundary condition (2) and the input constraint $|v_i(t)| \leq 1$, and we must show the existence of p satisfying the conditions (4)–(5). First, let

$$t_f = \sum_{j=1}^{\eta} T_j.$$

For $i < \eta$, we have

$$\begin{aligned} x_i(t_f) &= \zeta_i + \sum_{j=1}^{\eta} T_j \Upsilon_{ij} \widehat{U_j} \\ &= \zeta_i - \sum_{j=1}^{i-1} \left(\frac{\|\zeta_{j+1} - \zeta_j\|}{2} \right) \left(\frac{\zeta_{j+1} - \zeta_j}{\|\zeta_{j+1} - \zeta_j\|} \right) \\ &\quad + \sum_{j=i}^{\eta-1} \left(\frac{\|\zeta_{j+1} - \zeta_j\|}{2} \right) \left(\frac{\zeta_{j+1} - \zeta_j}{\|\zeta_{j+1} - \zeta_j\|} \right) \\ &\quad - \left(\frac{\|\zeta_1 + \zeta_\eta\|}{2} \right) \left(\frac{\zeta_1 + \zeta_\eta}{\|\zeta_1 + \zeta_\eta\|} \right) \\ &= \zeta_i - \left(\frac{\zeta_i - \zeta_1}{2} \right) + \left(\frac{\zeta_\eta - \zeta_i}{2} \right) - \left(\frac{\zeta_1 + \zeta_\eta}{2} \right) \\ &= 0, \end{aligned}$$

as desired. A similar computation verifies $x_\eta(t_f) = 0$. Next, we note that $|v_i(t)| \leq 1$ is trivially satisfied for $i \in \{1, \ldots, \eta\}$, since we have chosen $\Upsilon_{ij} = \pm 1$. Finally, if we define

$$p_i = \begin{cases} -\left(\widehat{U_\eta} + \widehat{U_1}\right)/2, & i = 1 \\ \left(\widehat{U_{i-1}} - \widehat{U_i}\right)/2, & i \in \{2, \ldots, \eta\} \end{cases}$$

then Lemma 6 tells us that

$$\begin{aligned} \{U_1, \ldots, U_\eta\} &= \arg \min_{u \in [0, \pi)} H(u) \\ 0 &= \min_{u \in [0, \pi)} H(u) \end{aligned}$$

and

$$\Upsilon_{ij} = -\text{sign}\left(p_i^T \widehat{U_j}\right)$$

for $i, j \in \{1, \ldots, \eta\}$, so p satisfies the conditions (4)–(5) and our result follows. ∎

III. Sufficient Conditions

In Section II, we showed that the trajectory produced by the algorithm in Fig. 2 satisfies the necessary conditions for optimality given by the minimum principle and so is a candidate solution to the minimum-time optimal control problem (1)-(2). The value function (i.e., cost-to-go) associated with this trajectory was found to be

$$Q(x) = \text{perim}\left(\text{conv}\left(\{x_1, \ldots, x_n, -x_1, \ldots, -x_n\}\right)\right)/4.$$

We will now establish sufficient conditions for optimality by showing that Q is a viscosity solution to the Hamilton-Jacobi-Bellman equation

$$\min_{\substack{u \in [0, \pi) \\ |v_i| \leq 1}} H(x, \nabla Q, u, v) = 0. \tag{7}$$

This partial differential equation enforces a condition analogous to (5), but replaces the costate p by the gradient ∇Q in the Hamiltonian function. We will remind the reader precisely what a viscosity solution is in Section III-A. For now, it is enough to note that Q cannot possibly be a "normal" solution to (7) since it is not differentiable everywhere. The proof of our main result will follow in Sections III-B and C.

A. Nonsmooth Analysis

In this section, we will say what it means for Q to be a viscosity solution of the Hamilton–Jacobi–Bellman equation (7). This material comes from the field of nonsmooth analysis [26], [27]. The key idea is to extend our notion of a derivative to points x at which Q is not differentiable.

1) Generalized Derivatives: Consider a function

$$f(x) : \mathbb{R}^n \to \mathbb{R}$$

that is everywhere Lipschitz. The *generalized directional derivative* of f at x in the direction $v \in \mathbb{R}^n$ is

$$f^\circ(x, v) = \limsup_{\substack{y \to x \\ t \downarrow 0}} \frac{f(y + tv) - f(y)}{t}.$$

The *generalized gradient* of f at x is

$$\partial f(x) = \left\{ p \in \mathbb{R}^n : f^\circ(x, v) \geq p^T v \text{ for all } v \in \mathbb{R}^n \right\}.$$

The *super-differential* of f at x, denoted by $D^+ f(x)$, is

$$\left\{ p \in \mathbb{R}^n : \limsup_{y \to x} \frac{f(y) - f(x) - p^T(y - x)}{\|y - x\|} \leq 0 \right\}.$$

The *sub-differential* of f at x, denoted by $D^- f(x)$, is

$$\left\{ p \in \mathbb{R}^n : \liminf_{y \to x} \frac{f(y) - f(x) - p^T(y - x)}{\|y - x\|} \geq 0 \right\}.$$

We note the following results, taken from [26] and [27]:

Lemma 8: Consider the continuous real-valued function $f : S \to \mathbb{R}$ defined on some open set $S \subset \mathbb{R}^n$.

1) If f is differentiable at $x \in S$, then
$$D^+ f(x) = D^- f(x) = \{\nabla f(x)\}.$$
2) If both $D^+ f(x)$ and $D^- f(x)$ are non-empty, then f is differentiable at x.
3) At any $x \in S$, we have
$$D^- f(x) \subset \partial f(x).$$
4) Let $\Omega \subset S$ be a set of points at which f is differentiable, and let $x \in S \setminus \Omega$. If $S \setminus \Omega$ has zero measure in S, then
$$\partial f(x) = \text{conv} \left(\left\{ \lim_{\substack{y \to x \\ y \in \Omega}} \nabla f(y) \right\} \right).$$
5) At any $x \in S$, we have $p \in D^- f(x)$ if and only if there exists a continuously differentiable function $g : S \to \mathbb{R}$ such that $p = \nabla g(x)$ and that $f - g$ has a local minimum at x.

These results will facilitate the process of actually computing generalized derivatives.

2) Viscosity Solutions: Now, we return to the Hamilton–Jacobi–Bellman equation (7). We say that Q is a *viscosity supersolution* of (7) if

$$\min_{\substack{u \in [0, \pi) \\ |v_i| \leq 1}} H(x, p, u, v) \geq 0 \tag{8}$$

for every $x \in \mathbb{R}^n$ and $p \in D^- Q(x)$. We say that Q is a *viscosity subsolution* of (7) if

$$\min_{\substack{u \in [0, \pi) \\ |v_i| \leq 1}} H(x, p, u, v) \leq 0 \tag{9}$$

for every $x \in \mathbb{R}^n$ and $p \in D^+ Q(x)$. We say that Q is a *viscosity solution* if it is both a viscosity supersolution and a viscosity subsolution. We recall (see, for example, [27, Sec. 8.7]) that any such Q is unique. As a consequence, if we can find a viscosity solution Q to (7), and if we can find a control policy that achieves $Q(x)$ for any set of initial conditions $x \in \mathbb{R}^2 \times \cdots \times \mathbb{R}^2$, then this control policy is optimal.

B. Solving the Hamilton–Jacobi–Bellman Equation

In this section we will verify the conditions (8)-(9) and so prove that Q is a viscosity solution of (7). We will abbreviate

$$\mathcal{X} = \mathbb{R}^2 \times \cdots \times \mathbb{R}^2.$$

Lemma 1 tells us that the following result is sufficient:

Lemma 9: If $p \in D^- Q(x)$ for some $x \in \mathcal{X}$, then

$$\min_{u \in [0, \pi)} \left(1 - \sum_{i=1}^{n} \left| p_i^T \widehat{u} \right| \right) \geq 0. \tag{10}$$

Similarly, if $p \in D^+ Q(x)$ for some $x \in \mathcal{X}$, then

$$\min_{u \in [0, \pi)} \left(1 - \sum_{i=1}^{n} \left| p_i^T \widehat{u} \right| \right) \leq 0. \tag{11}$$

Proof: Our proof will proceed as follows. First, we will express the value function Q in an explicit form that makes the analysis easier (see Section III-B1). Second, we will construct the set of points $\Omega \subset \mathcal{X}$ at which Q is differentiable, will find

$$D^+ Q(x) = D^- Q(x) = \{\nabla Q(x)\}$$

at any such point $x \in \Omega$, and will show that (10)–(11) are both satisfied there by the singleton $p = \nabla Q(x)$ (see Section III-B2). Third, we will show that $D^+ Q(x)$ is empty everywhere else, and so (11) holds trivially for $x \in \mathcal{X} \setminus \Omega$ (see Section III-B3). Finally, we will compute a superset $\partial Q(x) \supset D^- Q(x)$ for $x \in \mathcal{X} \setminus \Omega$, and complete our proof by verifying that (10) holds for all $p \in \partial Q(x)$ (see Section III-B4). ■

1) Form of the Value Function: The value of Q is invariant under reflection

$$x_i' = -x_i$$

for any i and reordering

$$x_i' = x_j, \qquad x_j' = x_i$$

for any i and j. So, we are free to assume that $x_1, \ldots, x_m$ are vertices of the convex hull

$$\text{conv}\left(\{x_1, \ldots, x_n, -x_1, \ldots, x_n\} \right)$$

for some $m \leq n$, and that $x_{m+1}, \ldots, x_n$ are not vertices of this convex hull. We are also free to assume that $x_1, \ldots, x_m$ are ordered counter-clockwise about the origin, that

$$\begin{bmatrix} 0 \\ 1 \end{bmatrix}^T x_i \geq \begin{bmatrix} 0 \\ 1 \end{bmatrix}^T x_1$$

for all $i \in \{1, \ldots, m\}$, and that

$$\begin{bmatrix} 0 \\ 1 \end{bmatrix}^T x_m = -\begin{bmatrix} 0 \\ 1 \end{bmatrix}^T x_1$$

if and only if $x_i = x_j$ for all $i, j \in \{1, \ldots, m\}$. We may then write

$$Q(x) = \frac{1}{2}\left(\|x_1 + x_m\| + \sum_{i=1}^{m-1} \|x_{i+1} - x_i\| \right).$$

2) Gradient of the Value Function: The set of all points at which Q is differentiable is

$$\Omega = \{x \in \mathcal{X} : x_i \neq x_{i+1} \text{ for all } i \in \{1, \ldots, m-1\}\}.$$

Let $x \in \Omega$. Then, we have

$$\frac{\partial Q}{\partial x_i} = \begin{cases} \frac{1}{2}\left(\frac{x_1 - x_2}{\|x_1 - x_2\|} + \frac{x_1 + x_m}{\|x_i + x_m\|} \right), & i = 1 \\ \frac{1}{2}\left(\frac{x_i - x_{i+1}}{\|x_i - x_{i+1}\|} + \frac{x_i - x_{i-1}}{\|x_i - x_{i-1}\|} \right), & 1 < i < m \\ \frac{1}{2}\left(\frac{x_m + x_1}{\|x_m + x_1\|} + \frac{x_m + x_{m-1}}{\|x_m - x_{m-1}\|} \right), & i = m \\ 0, & i > m. \end{cases}$$

Define $u_1, \ldots, u_m \in [0, \pi)$ such that

$$\widehat{u_i} = \begin{cases} (x_{i+1} - x_i) / \|x_{i+1} - x_i\|, & i < m \\ (x_1 + x_m) / \|x_1 + x_m\|, & i = m \end{cases}$$

so we may express

$$\frac{\partial Q}{\partial x_i} = \begin{cases} -(\widehat{u_m} + \widehat{u_1})/2, & i = 1 \\ (\widehat{u_{i-1}} - \widehat{u_i})/2, & 1 < i \leq m \\ 0, & i > m. \end{cases}$$

We take the convention

$$\nabla Q = \left[\begin{array}{ccc} \frac{\partial Q}{\partial x_1}^T & \cdots & \frac{\partial Q}{\partial x_n}^T \end{array} \right]^T$$

and recall from Lemma 8 that

$$D^- Q(x) = D^+ Q(x) = \{\nabla Q(x)\}.$$

Let $p = \nabla Q(x)$. Lemma 6 implies

$$\min_{u \in [0,\pi)} \left(1 - \sum_{i=1}^{n} \left| p_i^T \widehat{u} \right| \right) = 0.$$

So, results (10)–(11) hold whenever $x \in \Omega$.

3) Super-Differentials of the Value Function: Let $y \in \mathcal{X} \setminus \Omega$. Define $\mathcal{I} \subset \{1, \ldots, n\}$ such that

$$\{y_1, \ldots, y_n, -y_1, \ldots, -y_n\} = \{\pm y_i : i \in \mathcal{I}\}$$

and that $y_i \neq y_j$ for all $i, j \in \mathcal{I}$ satisfying $i \neq j$. Using this index set, define the function

$$Q'(x) = \text{perim}\left(\text{conv}\left(\{\pm x_i : i \in \mathcal{I}\}\right)\right)/4.$$

It is clear that $Q'(x)$ is differentiable at y. It is also clear that $Q'(x) - Q(x)$ has a local minimum at y, since $Q'(y) = Q(y)$ by construction and—because increasing the size of a point set can only increase the perimeter of its convex hull—we have $Q'(x) \geq Q(x)$ for all $x \in \mathcal{X}$. If we define $p = \nabla Q'(y)$, then Lemma 8 implies that $p \in D^- Q(y)$. As an immediate consequence, we can say that $D^- Q(x)$ is non-empty, hence from Lemma 8 that $D^+ Q(x)$ is empty, for all $x \in \mathcal{X} \setminus \Omega$. It is trivially the case, therefore, that result (11) holds whenever $x \in \mathcal{X} \setminus \Omega$, hence for all $x \in \mathcal{X}$.

4) Sub-Differentials of the Value Function: Let $x \in \mathcal{X} \setminus \Omega$. Recall from Lemma 8 that

$$D^- Q(x) \subset \partial Q(x) = \text{conv}\left(\left\{ \lim_{\substack{y \to x \\ y \in \Omega}} \nabla Q(y) \right\} \right).$$

Any limit point

$$q = \lim_{\substack{y \to x \\ y \in \Omega}} \nabla Q(y)$$

can be expressed as

$$q = \nabla Q(y')$$

for some $y' \in \Omega$ sufficiently close to x. In other words, there always exists some $y' \in \Omega$ at which

$$q_i = \left. \frac{\partial Q}{\partial x_i} \right|_{x = y'}$$

for all $i = 1, \ldots, n$. Since $\partial Q(x) \subset \mathbb{R}^n$, any $p \in \partial Q(x)$ can therefore be expressed as the convex combination

$$p = \sum_{j=1}^{n+1} a_j q^j$$

of $n+1$ limit points $q^1, \ldots, q^{n+1}$, where each $a_j \geq 0$, and

$$1 = \sum_{j=1}^{n+1} a_j.$$

We have already established that

$$\sum_{i=1}^{n} \left| {q_i^j}^T \widehat{u} \right| \geq 1$$

for all $j \in \{1, \ldots, n+1\}$ and $u \in [0, \pi)$. We compute

$$\begin{aligned} &\min_{u \in [0,\pi)} \left(1 - \sum_{i=1}^{n} \left| p_i^T \widehat{u} \right| \right) \\ &\quad = \min_{u \in [0,\pi)} \left(1 - \sum_{i=1}^{n} \left| \left(\sum_{j=1}^{n+1} a_j q_i^j \right)^T \widehat{u} \right| \right) \\ &\quad = \min_{u \in [0,\pi)} \left(1 - \sum_{i=1}^{n} \sum_{j=1}^{n+1} a_j \left| {q_i^j}^T \widehat{u} \right| \right) \\ &\quad = \min_{u \in [0,\pi)} \left(1 - \sum_{j=1}^{n+1} a_j \sum_{i=1}^{n} \left| {q_i^j}^T \widehat{u} \right| \right) \\ &\quad \geq \min_{u \in [0,\pi)} \left(1 - \sum_{j=1}^{n+1} a_j \, (1) \right) = 0. \end{aligned}$$

So, result (10) holds whenever $x \in \mathcal{X} \setminus \Omega$, hence for all $x \in \mathcal{X}$.

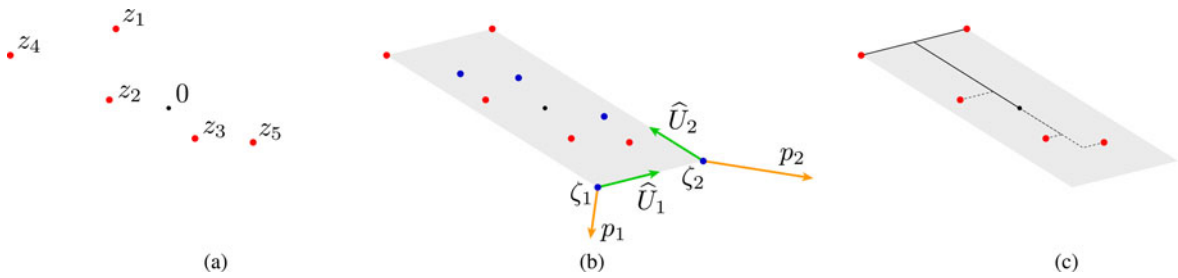

Fig. 3. Construction of a minimum-time optimal trajectory for five robots using the algorithm in Fig. 2. (a) The initial positions. (b) The convex hull of $\{z_1, \ldots, z_5, -z_1, \ldots, -z_5\}$. The optimal inputs U_1 and U_2 are aligned with the edges of this convex hull. (c) The resulting 2-step optimal trajectory.

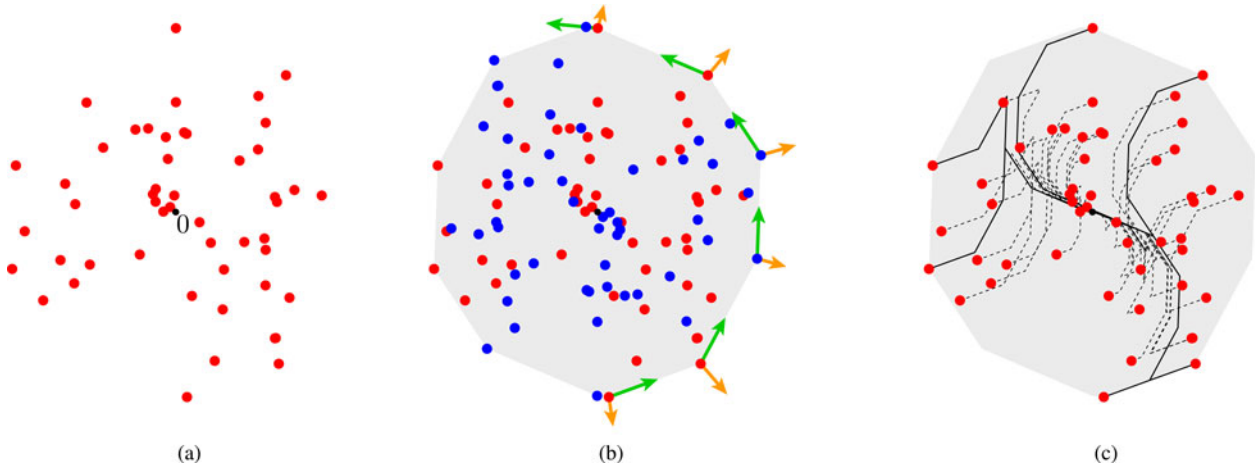

Fig. 4. Construction of an optimal trajectory for fifty robots. (a) The initial positions. (b) The convex hull of $\{z_1, \ldots, z_{50}, -z_1, \ldots, -z_{50}\}$. It has 12 vertices, implying six optimal inputs U_i (green arrows) associated with six costates p_i (orange arrows). (c) The resulting 6-step optimal trajectory.

C. Proof of Optimality

We have arrived at our main result:

Lemma 10: The η-step trajectory (T, U, V) produced by the algorithm OPTIMALCONTROL$(z_1, \ldots, z_n)$ in Fig. 2 is optimal for the problem (1)–(2).

Proof: It suffices to show that Q is a viscosity solution to (7) and that the trajectory produced by OPTIMALCONTROL achieves $t_f = Q(z)$ for any $x(0) = z$. The first result is provided by Lemma 9 and the second by Lemma 7. ■

IV. EXAMPLES

Having now shown that the trajectory produced by our algorithm OPTIMALCONTROL (see Fig. 2) is optimal for the problem (1)–(2), we will proceed to consider four examples in simulation. The first two examples (see Section IV-A) should make clear how the algorithm works. The third example (see Section IV-B) provides a bound on the worst-case cost t_f that is useful for design. The fourth example (see Section IV-C) shows how to consider obstacle avoidance while retaining optimality.

A. Computing Optimal Trajectories

Fig. 3 shows the construction of a minimum-time optimal trajectory for five robots, using the algorithm in Fig. 2. The first step of the algorithm is to reflect the initial positions across the origin and to compute the convex hull of the result. In this case, only two robots (index 1 and 4) start at vertices of conv $(\{z_1, \ldots, z_5, -z_1, \ldots, -z_5\})$, and so only these two robots have any effect on the optimal trajectory—we could simply ignore the others and arrive at the same result. As a consequence, the optimal trajectory has only two steps, with movement directions $\widehat{U}_1$ and $\widehat{U}_2$ that are aligned with edges of the convex hull. The costates p_1 and p_2 shown in Fig. 3(b) were the key to our proof of optimality: they led both to the necessary conditions we presented in Section II and—when interpreted as the gradient $p = \partial Q / \partial x$ of the value function—to the sufficient conditions we presented in Section III.

Fig. 4 shows the construction of an optimal trajectory for fifty robots, using the same approach. Despite the large number of robots, the convex hull conv $(\{z_1, \ldots, z_{50}, -z_1, \ldots, -z_{50}\})$ has only twelve vertices, so the optimal trajectory is again easy to compute and has a simple geometric structure.

In general, computing the optimal trajectory for n robots requires time $O(n \log n)$, which is exactly the time required to compute conv$\{z_1, \ldots, z_n, -z_1, \ldots, -z_n\}$. As the two examples in this section demonstrate, however, the "complexity" of the trajectory itself—as measured by the number of steps—is likely to be much smaller than n. In particular, if $z_1, \ldots, z_n$ are sampled uniformly in the unit disc, then the expected number of steps in the resulting optimal trajectory—i.e., the expected

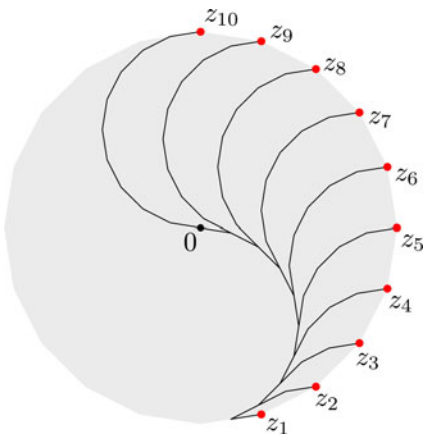

Fig. 5. Optimal trajectory for $n = 10$ robots that begin at vertices of a regular polygon with some radius $r > 0$. The cost of this trajectory is $t_f = r\,(n \sin(\pi/2n))$, which approaches $r(\pi/2)$ as $n \to \infty$, providing a simple bound on the worst-case "cost of coupling."

number of vertices in conv$\{z_1, \ldots, z_n, -z_1, \ldots, -z_n\}$—will converge asymptotically to $n^{1/3}$ [33].

B. Worst-Case Cost

Fig. 5 shows an optimal trajectory for $n = 10$ robots with initial positions

$$z_i = r \begin{bmatrix} \cos\left(\dfrac{i\pi}{n} - \dfrac{\pi}{2}\right) \\ \sin\left(\dfrac{i\pi}{n} - \dfrac{\pi}{2}\right) \end{bmatrix}$$

for $i \in \{1, \ldots, n\}$ and some $r > 0$. In this case

$$\text{conv}\left(\{z_1, \ldots, z_n, -z_1, \ldots, -z_n\}\right)$$

is a regular polygon with $2n$ sides, and so we easily compute

$$t_f = r\,(n \sin(\pi/2n))\,.$$

As $n \to \infty$, this cost converges asymptotically to $t_f = r(\pi/2)$, and indeed, this example makes clear that in general

$$\begin{aligned} t_f &= \text{perim}\left(\text{conv}\left(\{z_1, \ldots, z_n, -z_1, \ldots, -z_n\}\right)\right)/4 \\ &\leq \frac{\pi}{2}\left(\max_{i \in \{1,\ldots,n\}} \|z_i\|\right) \end{aligned}$$

for any choice of $z_1, \ldots, z_n \in \mathbb{R}^2$. If each robot was free to move in any direction, this cost would instead be

$$t_f = \max_{i \in \{1,\ldots,n\}} \|z_i\|$$

since robots would simply move along a straight line to the origin. As a consequence, with respect to our model, the design compromise that couples the movement direction of the microrobots in [1]–[6] only makes these robots $\pi/2$ times slower in worst case. This result is useful when deciding if it is worth the effort to eliminate coupling through further hardware modification.

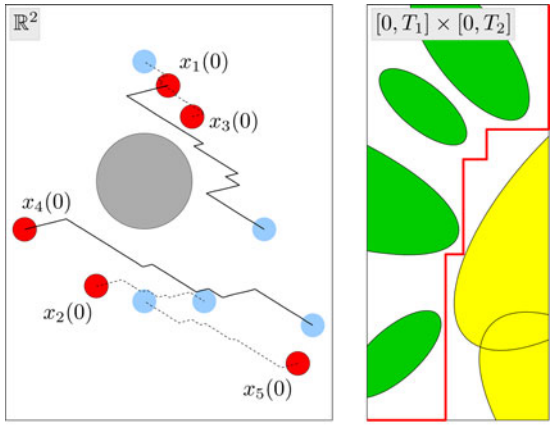

Fig. 6. Optimal trajectory for five robots that is also collision-free, as a direct extension of the example in Fig. 3. (a) The workspace $\mathbb{R}^2$. Both the robots (red) and the obstacle (gray) are circular in shape. The final position of each robot is shaded blue. Solid lines are paths followed by robots i for which z_i is a vertex of conv$(\{z_1, \ldots, z_5, -z_1, \ldots, -z_5\})$. Dotted lines are paths followed by other robots. (b) The coordination space $[0, T_1] \times [0, T_2]$. The red line is the function $\tau(t)$ that produces the workspace trajectory in (a) by $x_i(t) = x_i(0) + \tau_1 V_{i1} \widehat{U}_1 + \tau_1 V_{i2} \widehat{U}_2$. Green ellipses are regions of self-collision; yellow ellipses are regions of collision with the obstacle.

C. Collision Avoidance

The trajectory produced by the algorithm in Fig. 2 is not, in general, a unique solution to (1)–(2). For example, this algorithm tells us to apply the inputs $u(t) = U_1$ and $v_i = V_{i1}$ for time T_1, then $u(t) = U_2$ and $v_i = V_{i2}$ for time T_2, and so forth. The total cost would remain unchanged if we applied $u(t) = U_1$ and $v_i = V_{i1}$ for some fraction of time cT_1, where $0 \leq c \leq 1$, proceeded with the rest of the trajectory, and then returned at the end to apply $u(t) = U_1$ and $v_i = V_{i1}$ for time $(1 - c)T_1$. In fact, an optimal trajectory is produced by any continuous vector-valued function

$$\tau(t) : [0, t_f] \to [0, T_1] \times \cdots \times [0, T_\eta]$$

satisfying

$$\left.\begin{aligned} \tau_i(0) &= 0 \\ \tau_i(t_f) &= T_i \end{aligned}\right\} \text{ for } i \in \{1, \ldots, \eta\} \tag{12}$$

and

$$\frac{d\tau_i}{dt}(t) = \begin{cases} 1, & \text{for some } i \in \{1, \ldots, n\} \\ 0, & \text{for all other } i \end{cases} \tag{13}$$

for all $t \in [0, t_f]$ at which τ is differentiable. When $\eta = n$, the space of all such τ is exactly the space of all possible optimal trajectories. (When $\eta < n$, there are even more possibilities, but we will ignore them here for simplicity.) This space is reminiscent of the "task-completion diagram" or "coordination space" that has been used in multi-robot motion planning [28]–[30]. We can use it to consider obstacle avoidance while retaining a guarantee of optimality.

In particular, Fig. 6 shows an optimal trajectory for five robots that avoids both self-collision and collision with a single obstacle, assuming that both the robots and the obstacle are circular in shape. This trajectory is optimal for exactly the same problem

that we considered in Fig. 3—here, we have simply taken arbitrary $x_i(0)$ and $x_i(t_f)$ satisfying $z_i = x_i(0) - x_i(t_f)$ for $i \in \{1, \ldots, n\}$. As we saw in Fig. 3, the solution (T, U, V) that is returned by OPTIMALCONTROL has two steps, so collision-free optimal trajectories are captured by collision-free paths through $[0, T_1] \times [0, T_2]$ that satisfy (12)–(13). One such path is shown in Fig. 6(b), corresponding to the optimal trajectory in Fig. 6(a). Any classical motion planning algorithm can be used to find this path—in this case, we implemented a single-query, bidirectional, probabilistic roadmap algorithm similar to the one found in [34]. However, note that obstacles in $[0, T_1] \times \cdots \times [0, T_\eta]$ exhibit a lot of structure: circular obstacles in the workspace become ellipses in this "coordination space," precisely because for all $i \in \{1, \ldots, n\}$ there exist $b_i \in \mathbb{R}^2$ and $A_i \in \mathbb{R}^{2\times\eta}$ such that $x_i(t) = b_i + A_i\tau(t)$, or in other words x is a linear function of τ. Taking advantage of this structure is an opportunity for future work.

Note that there is no guarantee an optimal trajectory exists that is also collision-free. We view our approach as a strategy for local connection between nearby waypoints, perhaps used as a subroutine by a higher-level planner.

V. CURRENT LIMITATIONS AND FUTURE WORK

Our results in this paper have so far been entirely theoretical. Here, we consider how these results might apply in practice. We begin by acknowledging that our model (1)–(2) of the "Mag-Mite" robots in [1]–[6] is an abstraction. For example, we ignore the details of the resonant actuators that power these robots. These actuators are driven by a time-varying magnetic field that induces oscillatory impacts, the effect of which is modulated by surface friction and electrostatic clamping. Similarly, we assume that the orientation of the applied magnetic field—and, by extension, of the robots—can jump instantaneously. While this is a good approximation under slow switching, it may become a very bad approximation under rapid switching, since in practice there is some maximum rate at which the field orientation can be changed. Finally, it is clear that (1)–(2) is not necessarily a good model of any other microrobotic system, e.g., the untethered scratch-drive actuator [8] or the "Mag-μBot" [9], [10]. We briefly address some of these limitations as follows.

1) Dealing with uncertainty: It is possible to implement our optimal control law (see Fig. 2) as a state feedback policy, which may help reject disturbances and model perturbations encountered in practice (e.g., related to the resonant actuators). We have a closed-form expression for the value function $Q(x)$, so any choice of inputs u and $v_1 \ldots, v_n$ that achieve the minimum in (8) for some $p \in D^- Q(x)$ are optimal. These inputs can be found by maintaining the convex hull

$$\mathcal{C}(t) = \text{conv}\left(\{x_1(t), \ldots, x_n(t), -x_1(t), \ldots, -x_n(t)\}\right)$$

and doing the following at each sample time.

1) Find adjacent vertices a and b of $\mathcal{C}(t)$, ordered counterclockwise, that maximize the edge length $\|b - a\|$.
2) Choose u such that

$$\widehat{u} = (b - a)/\left\|b - a\right\|.$$

3) Choose $v_i = -\text{sign}(x_i^T Rp)$ for $i \in \{1, \ldots, n\}$, where

$$p = (b + a)/\left\|b + a\right\|, \qquad R = \begin{bmatrix} 0 & -1 \\ 1 & 0 \end{bmatrix}.$$

We leave a proof of stability to future work.

2) Adding complexity to the model: Our analysis may extend to small changes in (1)–(2). For example, to handle rapid switching of field orientation, we might use the model

$$\dot{x}_i = v_i\widehat{u}, \qquad \text{for } i \in \{1, \ldots, n\}$$
$$\dot{u} = w$$

and restrict $|v_i| \leq |w| \leq 1$. The Hamiltonian becomes

$$H(x, u, p, q, v, w) = 1 + \sum_{i=1}^{n} p_i^T\,(v_i\widehat{u}) + qw$$

where we immediately see that

$$v_i = -\text{sign}\left(p_i^T\,\widehat{u}\right), \qquad w = -\text{sign}\,(q)$$

and that there are at most n values of u at which $\dot{q} = 0$. In the same way that solutions to (1)–(2) were concatenations of straight lines, solutions to this new problem are evidently concatenations of Reeds–Shepp curves [24]. The details, of course, remain to be worked out.

3) Generalizing to other systems: The time complexity of our solution algorithm is $O(n \log n)$, and in particular is dominated by the computation of a planar convex hull. This beautiful geometric result is not one that we anticipated, and not one that we expect will extend to other systems, or even to variants of (1)–(2) like the one we consider above. However, understanding why this result emerged may be the key to generalizing our approach. We do not have a complete answer to this question, but believe it relates to the geometry of reachable sets. Robots in (1)–(2) are coupled by the choice of input $u(t)$. Given piecewise-constant $u(t)$, the reachable set for each robot is a copy of the same symmetric polygon. The optimal choice of $u(t)$ is evidently the one producing the "smallest" reachable set—in this case, the symmetric polygon with minimum perimeter—that contains $z_1, \ldots, z_n$. This polygon is conv $(\{z_1, \ldots, z_n, -z_1, \ldots, -z_n\})$. It would not be surprising if this line of thinking produced a much simpler geometric proof of our results in this paper. Generalizing this approach to other models of other systems might require only an explicit representation of the corresponding reachable sets. Even when these reachable sets are non-convex or hard to compute exactly, a convex relaxation may provide an approximate method of computation. These ideas are speculative, but we hope that some of them will be explored in future work.

APPENDIX

Our main result in this section is Lemma 13, which is necessary in the proof of Lemma 2 in Section II. We will first prove two supporting Lemmas. The mathematics required throughout this section come from elementary real analysis [35].

Lemma 11: Consider a function $g(u) : \mathbb{R} \to \mathbb{R}$ for which

$$g(u_0) = 0, \qquad \frac{dg}{du}(u_0) \neq 0$$

at some point $u_0 \in \mathbb{R}$. Then, for any $\epsilon_g > 0$ such that

$$\epsilon_g < \left| \frac{dg}{du}(u_0) \right|$$

there exists $\delta_g > 0$ such that $|g(u)| \geq \epsilon_g |u - u_0|$ whenever $|u - u_0| < \delta_g$.

Proof: For any $\epsilon > 0$, there exists $\delta > 0$ such that

$$\left| g(u) - g(u_0) - \frac{dg}{du}(u_0)(u - u_0) \right| \leq \epsilon |u - u_0| \tag{14}$$

whenever $|u - u_0| < \delta$. From the reverse triangle inequality and using the fact that $g(u_0) = 0$, (14) implies

$$|g(u)| - \left| \frac{dg}{du}(u_0)(u - u_0) \right| \geq -\epsilon |u - u_0|$$

or equivalently

$$|g(u)| \geq \left(\left| \frac{dg}{du}(u_0) \right| - \epsilon \right) |u - u_0|$$

For any $\epsilon_g > 0$ such that $\epsilon_g < |dg(u_0)/du|$, take

$$\epsilon = \left| \frac{dg}{du}(u_0) \right| - \epsilon_g$$

and we have our result. ∎

Lemma 12: Consider a function $h(u) : \mathbb{R} \to \mathbb{R}$ that is differentiable at some point $u_0 \in \mathbb{R}$. Then for any $\epsilon_h > 0$ there exists $\delta_h > 0$ such that $h(u) \geq h(u_0) - \epsilon_h |u - u_0|$ whenever $|u - u_0| < \delta_h$. If, in addition, this function satisfies

$$\frac{dh}{du}(u_0) \neq 0$$

then we may also ensure

$$\text{sign}\,(u - u_0) = \text{sign}\left(\frac{dh}{du}(u_0) \right).$$

Proof: For any $\epsilon > 0$ there exists $\delta > 0$ such that

$$\left| h(u) - h(u_0) - \frac{dh}{du}(u_0)(u - u_0) \right| \leq \epsilon |u - u_0| \tag{15}$$

whenever $|u - u_0| < \delta$. Equation (15) implies that

$$h(u) \geq h(u_0) + \frac{dh}{du}(u_0)(u - u_0) - \epsilon |u - u_0|.$$

If $dh(u_0)/du = 0$, then taking $\epsilon = \epsilon_h$ we immediately have our result. If $dh(u_0)/du \neq 0$, then requiring

$$\text{sign}\,(u - u_0) = \text{sign}\left(\frac{dh}{du}(u_0) \right)$$

ensures

$$h(u) \geq h(u_0) + \left(\left| \frac{dh}{du}(u_0) \right| - \epsilon \right) |u - u_0|,$$

so taking

$$\epsilon = \left| \frac{dh}{du}(u_0) \right| + \epsilon_h$$

again produces our result. ∎

We are now ready to prove our main result.

Lemma 13: If $g(u), h(u) : \mathbb{R} \to \mathbb{R}$ are both differentiable at $u_0 \in \mathbb{R}$ and if

$$g(u_0) = \quad \frac{dg}{du}(u_0) \neq 0,$$

then $f(u) = |g(u)| + h(u)$ has no maximum at $u_0 \in \mathbb{R}$.

Proof: Lemmas 11-12 tell us that for any $\epsilon = \epsilon_g - \epsilon_h > 0$ satisfying $\epsilon < |dg(u_0)/du|$, there exists $\delta = \min\{\delta_g, \delta_h\}$ such that

$$\begin{aligned} f(u) &\geq \epsilon_g |u - u_0| + h(u_0) - \epsilon_h |u - u_0| \\ &= f(u_0) + (\epsilon_g - \epsilon_h) |u - u_0| \\ &= f(u_0) + \epsilon |u - u_0| \end{aligned}$$

whenever $|u - u_0| < \delta$ and

$$\text{sign}\,(u - u_0) = \text{sign}\left(\frac{dh}{du}(u_0) \right)$$

if $dh(u_0)/du \neq 0$. This result implies that we can always find nearby $u_1 \neq 0$ such that $f(u_1) \geq f(u_0)$, and so $f(u)$ has no maximum at u_0, as desired. ∎

ACKNOWLEDGMENT

The author thanks the anonymous reviewers for their insightful comments, as well as D. Frutiger, B. Kratochvil, B. Nelson, G. Arechavaleta, and S. Hutchinson for helpful discussions.

REFERENCES

[1] D. R. Frutiger, K. Vollmers, B. E. Kratochvil, and B. J. Nelson, "Small, fast, and under control: Wireless resonant magnetic micro-agents," *Int. J. Rob. Res.*, vol. 29, no. 5, pp. 613–636, 2010.

[2] B. Kratochvil, D. Frutiger, K. Vollmers, and B. Nelson, "Visual servoing and characterization of resonant magnetic actuators for decoupled locomotion of multiple untethered mobile microrobots," in *IEEE Int. Conf. Rob. Aut.*, May 2009, pp. 1010–1015.

[3] D. Frutiger, B. Kratochvil, and B. Nelson, "Magmites - microrobots for wireless microhandling in dry and wet environments," in *IEEE Int. Conf. Rob. Aut.*, May 2010, pp. 1112–1113.

[4] Z. Nagy, D. Frutiger, R. Leine, C. Glocker, and B. Nelson, "Modeling and analysis of wireless resonant magnetic microactuators," in *IEEE Int. Conf. Rob. Aut.*, May 2010, pp. 1598–1603.

[5] K. Vollmers, D. R. Frutiger, B. E. Kratochvil, and B. J. Nelson, "Wireless resonant magnetic microactuator for untethered mobile microrobots," *Applied Physics Letters*, vol. 92, no. 14, pp. 144 103–3, 2008.

[6] D. Frutiger, B. Kratochvil, K. Vollmers, and B. J. Nelson, "Magmites - wireless resonant magnetic microrobots," in *IEEE Int. Conf. Rob. Aut.*, Pasadena, CA, 2008.

[7] M. Sitti, "Microscale and nanoscale robotics systems [grand challenges of robotics]," *IEEE Robotics & Automation Magazine*, vol. 14, no. 1, pp. 53–60, Mar. 2007.

[8] B. R. Donald, C. G. Levey, C. D. McGray, I. Paprotny, and D. Rus, "An untethered, electrostatic, globally controllable MEMS micro-robot," *J. Microelectromech. Syst.*, vol. 15, no. 1, pp. 1–15, Feb. 2006.

[9] C. Pawashe, S. Floyd, and M. Sitti, "Modeling and experimental characterization of an untethered magnetic micro-robot," *Int. J. Rob. Res.*, vol. 28, no. 8, pp. 1077–1094, Aug. 2009.

[10] S. Floyd, C. Pawashe, and M. Sitti, "Two-dimensional contact and noncontact micromanipulation in liquid using an untethered mobile magnetic microrobot," *IEEE Trans. Robot.*, vol. 25, no. 6, pp. 1332–1342, Dec. 2009.

[11] B. R. Donald, C. G. Levey, I. Paprotny, and D. Rus, "Simultaneous control of multiple mems microrobots," in *WAFR*, 2008.

[12] B. R. Donald, C. G. Levey, and I. Paprotny, "Planar microassembly by parallel actuation of mems microrobots," *Journal of Microelectromechanical Systems*, vol. 17, no. 4, pp. 789–808, Aug. 2008.
[13] S. Floyd, C. Pawashe, and M. Sitti, "Microparticle manipulation using multiple untethered magnetic micro-robots on an electrostatic surface," in *Int. Conf. Int. Rob. Sys.*, Oct. 2009, pp. 528–533.
[14] T. Bretl, "Control of many agents with few instructions," in *Robotics: Science and Systems*, Atlanta, GA, June 2007.
[15] T. Bretl, "Control of many agents by moving their targets: Maintaining separation," in *Int. Conf. on Advanced Robotics*, Jeju, Korea, August 2007.
[16] A. Becker and T. Bretl, "Motion planning under bounded uncertainty using ensemble control," in *Robotics: Science and Systems (RSS)*, 2010.
[17] J. Ueda, L. Odhner, and H. H. Asada, "Broadcast feedback of stochastic cellular actuators inspired by biological muscle control," *Int. J. Rob. Res.*, vol. 26, no. 11–12, pp. 1251–1265, Nov. 2007.
[18] L. U. Odhner and H. Asada, "Stochastic recruitment control of large ensemble systems with limited feedback," *Journal of Dynamic Systems Measurement and Control*, vol. 132, no. 4, Jul. 2010.
[19] J.-S. Li and N. Khaneja, "Control of inhomogeneous quantum ensembles," *Physical Review A (Atomic, Molecular, and Optical Physics)*, vol. 73, no. 3, p. 030302, 2006.
[20] J.-S. Li and N. Khaneja, "Ensemble control of bloch equations," *IEEE Trans. Autom. Control*, vol. 54, no. 3, pp. 528–536, Mar. 2009.
[21] L. S. Pontryagin, V. G. Boltyanskii, R. V. Gamkrelidze, and E. F. Mishchenko, *The Mathematical Theory of Optimal Processes*. John Wiley, 1962.
[22] V. G. Boltyanskii, "Sufficient conditions for optimality and the justification of the dynamic programming method," *SIAM Journal on Control*, vol. 4, no. 2, pp. 326–361, 1966.
[23] L. E. Dubins, "On curves of minimal length with a constraint on average curvature, and with prescribed initial and terminal positions and tangents," *American Journal of Mathematics*, vol. 79, no. 3, pp. 497–516, 1957.
[24] J. A. Reeds and L. A. Shepp, "Optimal paths for a car that goes both forwards and backwards," *Pacific J. Math.*, vol. 145, pp. 367–393, 1990.
[25] D. J. Balkcom and M. T. Mason, "Time optimal trajectories for bounded velocity differential drive vehicles," *Int. J. Rob. Res.*, vol. 21, no. 3, pp. 199–217, 3 2002.
[26] F. H. Clarke, *Optimization and nonsmooth analysis*. New York: Wiley, 1983.
[27] A. Bressan and B. Piccoli, *Introduction to the mathematical theory of control*. American Institute of Mathematical Sciences, 2007.
[28] P. O'Donnell and T. Lozano-Perez, "Deadlock-free and collision-free coordination of two robot manipulators," in *IEEE Int. Conf. Rob. Aut.*, May 1989, pp. 484–489.
[29] S. LaValle and S. Hutchinson, "Optimal motion planning for multiple robots having independent goals," *IEEE Trans. Robot. Autom.*, vol. 14, no. 6, pp. 912–925, Dec. 1998.
[30] T. Simeon, S. Leroy, and J.-P. Lauumond, "Path coordination for multiple mobile robots: a resolution-complete algorithm," *IEEE Trans. Robot. Autom.*, vol. 18, no. 1, pp. 42–49, Feb. 2002.
[31] D. DeVon and T. Bretl, "Control of many agents moving in the same direction with different speeds: a decoupling approach," in *American Control Conference*, 2009.
[32] M. Athans and P. L. Falb, *Optimal Control: An Introduction to the Theory and Its Applications*. McGraw-Hill, 1966.
[33] A. Rényi and R. Sulanke, "Über die konvexe hülle von n zufällig gewählten punkten," *Probability Theory and Related Fields*, vol. 2, no. 1, pp. 75–84, 1963-01-01.
[34] G. Sánchez and J.-C. Latombe, "On delaying collision checking in PRM planning: Application to multi-robot coordination," *Int. J. Rob. Res.*, vol. 21, no. 1, pp. 5–26, 2002.
[35] H. L. Royden, *Real Analysis*, 3rd ed. Prentice Hall, 1988.

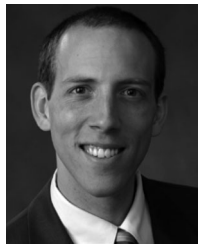

Timothy Bretl (S'02–M'05) received the B.S. degree in Engineering and the B.A. degree in Mathematics from Swarthmore College, Swarthmore, PA, in 1999 and the M.S. and Ph.D. degrees, both in aeronautics and astronautics, from Stanford University, Stanford, CA, in 2000 and 2005, respectively.

Subsequently, he was a Postdoctoral Fellow with the Department of Computer Science, Stanford University. Since 2006, he has been with the University of Illinois at Urbana-Champaign, where he is an Assistant Professor of Aerospace Engineering and a Research Assistant Professor with the Coordinated Science Laboratory.

Dr. Bretl received the National Science Foundation Faculty Early Career Development Award in 2010.